

# Rational Design of Proteolytically Stable, Cell-Permeable Peptide-Based Selective Mcl-1 Inhibitors

Avinash Muppidi,<sup>†</sup> Kenichiro Doi,<sup>‡</sup> Selvakumar Edwardraja,<sup>†</sup> Eric J. Drake,<sup>§</sup> Andrew M. Gulick,<sup>§</sup> Hong-Gang Wang,<sup>‡</sup> and Qing Lin<sup>\*,†</sup>

<sup>†</sup>Department of Chemistry, State University of New York at Buffalo, Buffalo, New York 14260-3000, United States

<sup>‡</sup>Department of Pharmacology, Pennsylvania State University College of Medicine, Hershey, Pennsylvania 17033, United States

<sup>§</sup>Hauptman-Woodward Institute and Department of Structural Biology, State University of New York at Buffalo, Buffalo, New York 14203, United States

## S Supporting Information

**ABSTRACT:** Direct chemical modifications provide a simple and effective means to “translate” bioactive helical peptides into potential therapeutics targeting intracellular protein–protein interactions. We previously showed that distance-matching bisaryl cross-linkers can reinforce peptide helices containing two cysteines at the *i* and *i*+7 positions and confer cell permeability to the cross-linked peptides. Here we report the first crystal structure of a biphenyl-cross-linked Noxa peptide in complex with its target Mcl-1 at 2.0 Å resolution. Guided by this structure, we remodeled the surface of this cross-linked peptide through side-chain substitution and N-methylation and obtained a pair of cross-linked peptides with substantially increased helicity, cell permeability, proteolytic stability, and cell-killing activity in Mcl-1-overexpressing U937 cells.

BH3-only proteins are pro-apoptotic factors that induce cell death through selective binding to anti-apoptotic Bcl-2 family proteins.<sup>1</sup> In a majority of cancers, interactions between pro-apoptotic BH3 proteins and anti-apoptotic Bcl-2 family proteins are deregulated because of elevated expression of some Bcl-2 family proteins such as Bcl-2, Bcl-x<sub>L</sub>, and Mcl-1,<sup>2</sup> which contributes to cancer progression and renders cancer cells resistant to chemo- and radiotherapy.<sup>3</sup> A proven strategy in cancer therapeutic development is to design BH3 mimics as selective Bcl-2 inhibitors.<sup>4</sup> Two approaches have been successfully employed: (i) the use of small molecules to mimic BH3 peptide side chains involved in binding<sup>5</sup> and (ii) chemical modification of BH3 peptides to improve their pharmaceutical properties.<sup>6</sup> In the former approach, a potent small-molecule Bcl-2 inhibitor, ABT-737, was designed<sup>7</sup> that binds tightly to Bcl-2 and Bcl-x<sub>L</sub> with sub-nM affinity but poorly to Mcl-1;<sup>8</sup> in the latter, chemically modified BH3 peptides containing  $\alpha/\beta$ -amino acid backbones,<sup>9</sup> side-chain cross-linking,<sup>10</sup> and main-chain-to-side chain cross-linking<sup>11</sup> showed improved cell permeability and/or serum stability.

Mcl-1 is a member of the Bcl-2 family that undergoes frequent somatic amplification in multiple cancers and functions as a key driver of cancer cell survival.<sup>12</sup> Although small-molecule Bcl-2-selective inhibitors (e.g., ABT-263) have entered clinical trials, they generally lack efficacy in tumors with elevated levels of Mcl-

1.<sup>13</sup> Since a NoxaB-(75–93)-C75A peptide derived from BH3-only Noxa protein binds to Mcl-1 with high affinity and selectivity,<sup>14</sup> an attractive approach for the development of Mcl-1-selective inhibitors is to optimize the pharmaceutical properties of Noxa BH3 peptide. We recently reported a new dicysteine alkylation-based side-chain cross-linking chemistry using a pair of distance-matching bisaryl cross-linkers that lead to reinforced peptide helices and improved cellular uptake.<sup>15</sup> Here we report the first crystal structure of a biphenyl-cross-linked Noxa BH3 peptide in complex with Mcl-1 and the subsequent design of a pair of proteolytically stable, cell-permeable, peptide-based Mcl-1 inhibitors by combining structure-based peptide side-chain cross-linking with peptide surface remodeling.

To apply our cysteine-mediated cross-linking chemistry to NoxaB-(75–93)-C75A peptide (hereafter called Noxa peptide), we replaced two solvent-exposed *i* and *i*+7 residues (Gln-77, Lys-84) in Noxa with D- or L-cysteine and subjected the 19-mer peptide to 4,4'-bis(bromomethyl)biphenyl (Bph)-mediated cross-linking (see Table S1 for peptide characterizations). The inhibitory activities of the cross-linked peptides were then evaluated using a competitive fluorescence polarization (FP) assay. Compared with the parent Noxa peptide, Bph-cross-linked peptides **1** and **2** showed 65- and 12-fold increases in inhibitory activity, respectively (Table 1). To verify that the Mcl-1 targeting selectivity remained intact after cysteine substitution and subsequent side-chain cross-linking, N-terminal fluorescein-conjugated, Bph-cross-linked Noxa peptides Fl-1 and Fl-2 were prepared, and their binding affinities toward Mcl-1 and Bcl-x<sub>L</sub> were measured using the FP assay. Gratifyingly, like Noxa, the cross-linked Noxa peptides showed comparable binding affinities toward Mcl-1 ( $K_d = 4.9 \pm 1.5$  nM for Fl-1,  $3.4 \pm 0.2$  nM for Fl-2 vs  $6.7 \pm 1.0$  nM for Noxa) but no measurable affinity toward Bcl-x<sub>L</sub> ( $K_d > 1000$  nM), indicating >200-fold selectivity for Mcl-1. As a control, the BH3 domain of the BH3-only protein Bim showed essentially equal potencies toward Mcl-1 and Bcl-x<sub>L</sub> in the same assay (Table S3). To our surprise, similar to the parent Noxa peptide, the cross-linked Noxa peptides **1** and **2** showed no activity in a cell viability assay in which Mcl-1-overexpressing U937 cells were treated with 20  $\mu$ M peptide for 48 h, suggesting

Received: July 13, 2012

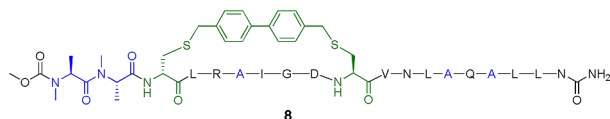
Published: August 25, 2012



**Table 1. Sequences and Biological Activities of the Native and Chemically Modified Noxa BH3 Peptides**

Name	Sequence <sup>a</sup>	Charge	FP assay <sup>b</sup> <i>K<sub>i</sub></i> (nM)	Cell viability <sup>c</sup> (%)
Noxa	AAQLRRIGDKVNLQRKLLN	+4	648±128	97.6±0.9
1	AAC'LRRIGDC'VNLQRKLLN <sup>d</sup>	+3	10±1	98.6±4.0
2	AAc'LRRIGDC'VNLQRKLLN <sup>e</sup>	+3	54±14	100.3±0.2
3	AAc'LRAIGDC'VNLQRKLLN	+2	23±8	85.9±2.2
4	AAc'LRAIGDC'VNLAQKLLN	+1	28±11	72.9±3.2
5	AAc'LRAIGDC'VNLAQALLN	0	29±4	44.3±0.2
6	A <sub>m</sub> Ac'LRRIGDC'VNLQRKLLN <sup>f</sup>	+3	32±3	87.3±2.8
7	A <sub>m</sub> A <sub>m</sub> c'LRRIGDC'VNLQRKLLN	+3	22±4	80.5±4.7
8	A <sub>m</sub> A <sub>m</sub> c'LRAIGDC'VNLAQALLN <sup>g</sup>	0	22±8	34.8±0.5

<sup>a</sup>Peptides with N-terminal Ala were acetylated; those with N-terminal N-methylalanine were capped with methoxycarbonyl; all were amidated at the C-terminus. <sup>b</sup>Competitive FP assay performed three times to derive *K<sub>i</sub>* values and standard deviations. <sup>c</sup>Cell viability measured with ATP assay by treating Mcl-1-overexpressing U937 cells (cultured in RPMI1640 supplemented with 5% fetal bovine serum) with 20 μM peptide for 48 h. <sup>d</sup>C' = Bph-linked L-cysteine. <sup>e</sup>C' = Bph-linked D-cysteine. <sup>f</sup>A<sub>m</sub> = N-methylalanine. <sup>g</sup>Structure of 8:



that Bph-mediated side-chain cross-linking is inefficient in allowing sufficient cytosolic transport.

To gain a structural understanding of how the cross-linked Noxa peptide binds to Mcl-1, we solved the crystal structure of mouse Mcl-1 (mMcl-1) in complex with **2** by molecular replacement. The structure was refined to 2.0 Å resolution with  $R_{\text{cryst}} = 19.2\%$  and  $R_{\text{free}} = 23.9\%$  (see Table S2 for crystal data and structural refinement). Overall, the Mcl-1 subunit in the complex is superimposable with the mMcl-1 NMR structure (PDB entry 2JM6) with a root-mean-square deviation of 1.2 Å (Figure S2).<sup>14</sup> Bound peptide **2** adopts a helical conformation, with the Bph cross-linker projecting 90° away from the deep hydrophobic binding groove (Figure 1a). Compared to 2JM6, most of the interactions between Noxa and mMcl-1 were maintained. A few H-bonds are formed only in the mMcl-1:2 complex, namely, those between the Noxa Asp-9 and mMcl-1 Asn-241 side chains and between the Noxa Arg-5 side chain and the mMcl-1 backbone His-233 and Val-234. In addition, the Bph cross-linker forms an edge-to-face  $\pi$ - $\pi$  interaction with His-205 of mMcl-1 (Figure 1a). When cross-linked peptide **2** was superimposed with the linear Noxa peptide in 2JM6, significant changes in the side-chain orientations in **2** were observed for the solvent-exposed, positively charged residues (Figure 1b). For example, the Arg-6 side chain is disengaged from the salt bridge with Asp-238 of mMcl-1 and reoriented toward the Bph cross-linker; Arg-14 becomes completely solvent-exposed, as the salt bridge with the mMcl-1 Gly-308 carboxyl terminus was not detected; and the Lys-16 side chain is disengaged from the salt bridge with the Noxa Met-20 carboxyl terminus as a result of the Noxa peptide truncation. Together, the results suggest that these three solvent-exposed, positively charged residues can be replaced without loss of binding affinity toward Mcl-1.

Since molecules with large polar surface areas generally show poor passive membrane permeation,<sup>16</sup> we hypothesized that

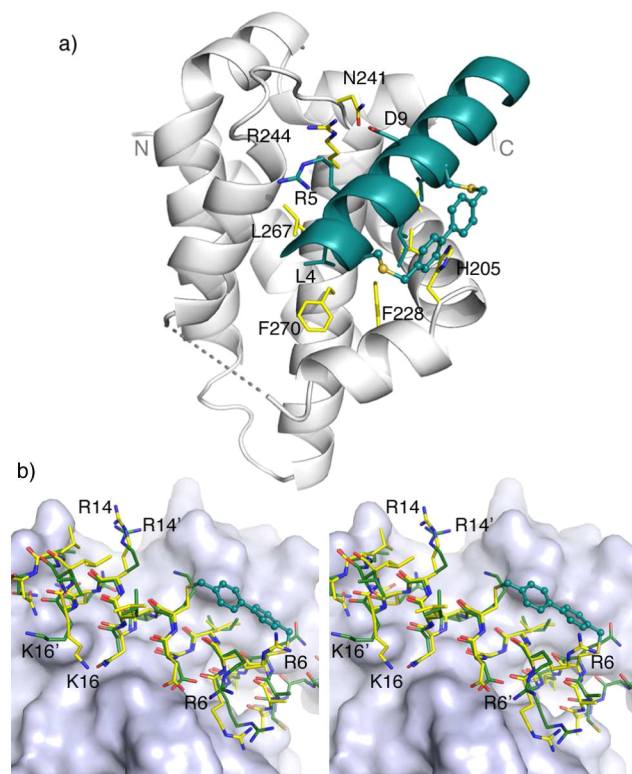


**Figure 1.** Crystal structure of mouse Mcl-1 in complex with Bph-cross-linked Noxa BH3 peptide **2**. (a) Overall complex structure. The peptide and the side chains of three canonical hydrophobic residues of peptide **2**, Leu-4 (h2), Ile-7 (h3), and Val-11 (h4), are colored in deep teal. The two flexible loops, Gly-173 to Gly-187 (in the front; shown as a dashed line) and Leu-216 to Val-224 (in the back; not shown), were disordered in the electron density maps. (b) Stereo view of superimposed Bph-cross-linked peptide **2** (yellow stick model) with mNoxa BH3 peptide (green stick model) as seen in 2JM6. The BH3-binding pocket of mMcl-1 is rendered as a surface model.

substituting the solvent-exposed charged residues with neutral ones would substantially improve the cell permeability of the cross-linked Noxa peptides, leading to increased cellular activity. Accordingly, we replaced one, two, or all three of the nonessential residues Arg-6, Arg-14, and Lys-16 in **2** with Ala to obtain cross-linked peptides **3**–**5**. We then assessed their inhibitory activities against Mcl-1 using competitive FP assay and their cell-killing activities in U937 cells using ATP assay (Table 1). To our satisfaction, a roughly 2-fold increase in inhibitory activity was observed after Ala substitution. More importantly, we observed progressive increases in cellular activity as the net charge decreased from +3 to 0, with only 44% of U937 cells remaining viable after treatment with charge-neutral cross-linked peptide **5** (20 μM). This implies that the charge-neutral peptide surface facilitates cytosolic transport of the cross-linked peptides, presumably through passive membrane diffusion. While **5** still has two charged residues, Arg-5 and Asp-9, which contribute to Mcl-1 binding (Figure 1a), it is tempting to speculate that they may form an internal salt bridge in the lipid bilayer during membrane transport because of their favorable *i*, *i*+4 geometry.

Encouraged by the initial Arg/Lys-to-Ala substitution results, we sought to further reduce the number of polar groups on the peptide surface to maximize passive membrane diffusion. In this regard, a proven modification is backbone N-methylation, especially for the N–H groups not involved in intramolecular H-bonding.<sup>17</sup> For the N-acyl-capped helical peptides, the first

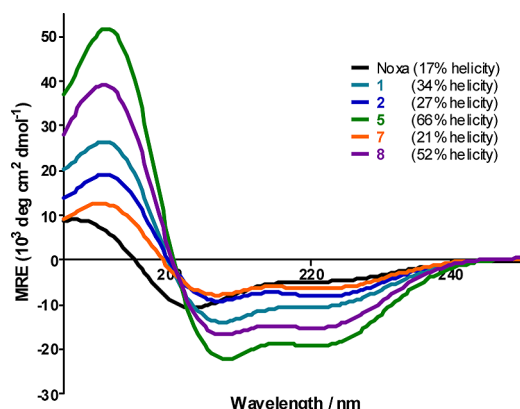


**Figure 2.** CD spectra of the Bph-cross-linked and linear Noxa peptides and their calculated percent helicities. The peptides were dissolved in 1:1 CH<sub>3</sub>CN/H<sub>2</sub>O at a final concentration of 50  $\mu$ M. The percent helicity was calculated using the  $[\theta]_{222}$  value.

three N-terminal N–H groups typically are not engaged in intramolecular H-bonding because of the lack of preceding carbonyl groups one helical turn away. Careful examination of the structure of the Mcl-1:2 complex reveals that the first two Ala N–H groups are solvent-exposed, while the third residue, D-Cys N–H, forms a H-bond with the capping acetyl group (H $\cdots$ O = 2.20 Å) (Figure S2c). We thus substituted one or both of the N-terminal alanines with N-methyl-Ala to generate the cross-linked peptides 6–8 and compared their inhibitory activities to that of their parent peptide (Table 1). We found that adding two N-methyl groups afforded higher activities in the FP and the cell viability assays (compare 7 to 2 and 8 to 5). In particular, Bph-cross-linked peptide 8 containing two N-methyl groups in addition to three Ala substitutions showed the most robust activity in cell culture: only 35% of the U937 cells remained viable after treatment with 8 for 48 h (Table 1). A concentration-dependent ATP assay for 8 using U937 cells gave rise to a half-maximal effective concentration of 13.4  $\mu$ M (Figure S3).

To probe the effect of chemical modifications on peptide secondary structure, we performed far-UV CD measurements and determined the helicities of cross-linked Noxa peptides 1, 2, 5, 7, and 8 along with the linear Noxa peptide (Figure 2). All of the Bph-cross-linked peptides had higher helicities than the linear Noxa peptide. Replacing the three positively charged residues with Ala in the cross-linked peptides led to a >2-fold increase in helicity (compare 5 to 2), presumably as a result of the stronger helix-formation propensity of Ala relative to Arg and Lys.<sup>18</sup> Adding two N-methyl groups at the N-terminus appeared to destabilize the helix (compare 7 to 2),<sup>19</sup> but the Ala-substituted, cross-linked peptide 8 seemed to tolerate N-methylation to some extent (52% helicity for 8 vs 66% for 5).

To confirm that the increased cellular activity was a result of improved cytosolic transport, we prepared fluorescein-labeled Bph-cross-linked peptides Fluo-2, Fluo-5, and Fluo-8, together with Fluo-Noxa (Table S1). The uptake of these cross-linked and linear peptides into HeLa cells at 37 and 4 °C was analyzed by fluorescence-activated cell sorting. We expected the energy-dependent active transport processes (e.g., pinocytosis, previously reported to be a major membrane permeation pathway for side-chain cross-linked peptides<sup>20</sup>) to be inhibited at 4 °C and the passive membrane diffusion to remain unaffected. Not surprisingly, we observed that Bph-mediated cross-linking enhanced peptide cellular uptake 26–40-fold at 37 °C and 7–33-fold at 4 °C (compare Fluo-2, -5, and -8 to Fluo-Noxa in Figure

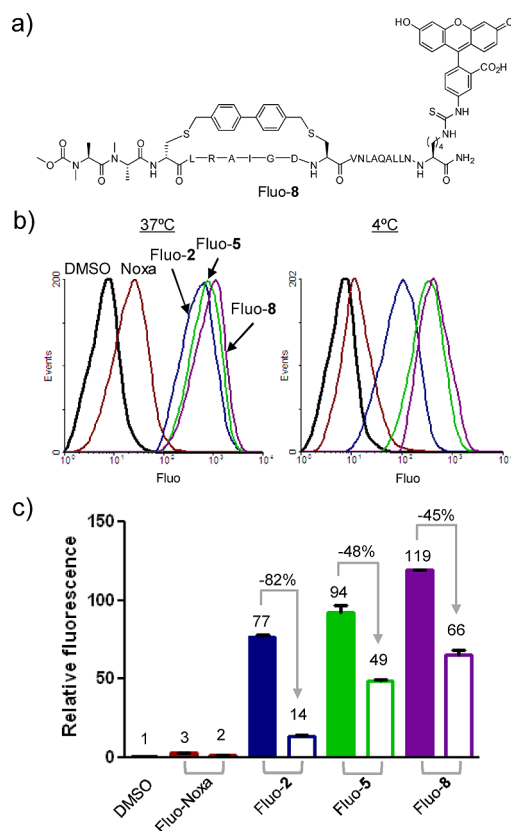


**Figure 3.** Flow cytometry analysis of HeLa cells after treatment with Fluo-Noxa, Fluo-2, Fluo-5, and Fluo-8 (10  $\mu$ M). (a) Structure of Fluo-8. (b) Representative flow cytometry histograms at 37 °C (left) and 4 °C (right). (c) Bar graph showing normalized relative fluorescence at 37 °C (filled) and 4 °C (open).

3b,c). However, the effect of the temperature switch from 37 to 4 °C varied: the +3 charged, cross-linked peptide 2 showed 82% reduction, whereas the Ala-substituted, charge-neutral cross-linked peptides showed much smaller reductions (48% for Fluo-5 and 45% for Fluo-8). The dramatic reduction in cellular uptake of Fluo-2 indicates that 2 permeates into cells mainly through the energy-dependent endocytotic process, resulting in endosome trapping. The smaller reductions for 5 and 8 indicate that passive membrane diffusion represents a major pathway for the uptake because of their favorable physicochemical properties, including neutral charge, reduced number of polar groups on their surfaces, and overall higher helicity. A confocal microscopy experiment confirmed that the cross-linked peptides 5 and 8 were predominantly localized in the cytosol and not bound to the cell membrane (Figure S4).

A key benefit of peptide side-chain cross-linking is improved proteolytic stability. To test this, we selected the most potent Bph-cross-linked peptides, 5 and 8, and compared their proteolytic stabilities to that of the parent Noxa peptide in the presence of chymotrypsin, trypsin, and mouse serum (Figure 4). In all three cases, 5 and 8 exhibited greatly improved proteolytic stabilities relative to the linear Noxa peptide: 8.7- and 7.2-fold improvements in half-life ( $t_{1/2}$ ) against chymotrypsin and 14.8- and 8.9-fold improvements against trypsin, respectively. The higher stability of 5 relative to 8 can be attributed to its higher helicity (66% vs 52%). The most dramatic effect was seen with mouse serum, where the linear Noxa peptide showed a  $t_{1/2}$  of only  $10.5 \pm 2.3$  min, while for 5 and 8  $t_{1/2} = 31.6 \pm 2.2$  and  $21.2 \pm$



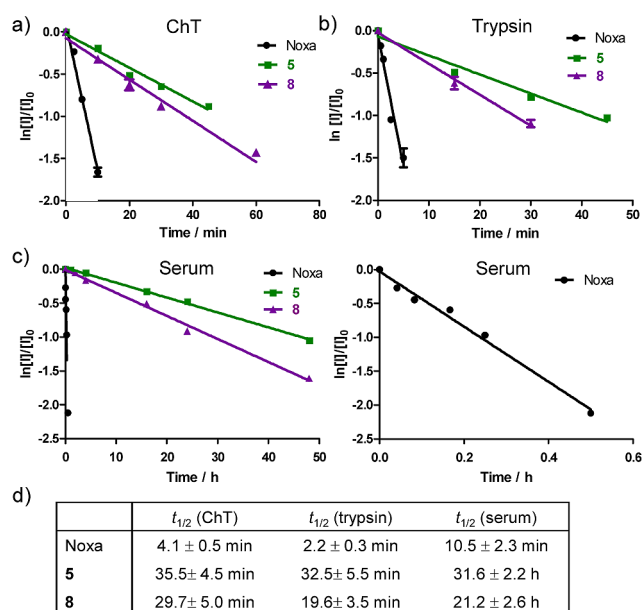


**Figure 4.** Proteolytic stabilities of the linear and Bph-cross-linked Noxa peptides in the presence of (a) chymotrypsin (ChT), (b) trypsin, and (c) mouse serum (with a zoom-in of the degradation plot for the linear Noxa peptide shown on the right). (d) Calculated average  $t_{1/2}$  values for the peptides. The measurements were performed three times for ChT and trypsin and twice for mouse serum.

2.6 h, representing 180- and 121-fold increases in stability, respectively. This prolonged stability may also be partly due to the presence of the hydrophobic biphenyl cross-linker in **5** and **8**, which facilitates sequestration/protection of the Bph-cross-linked peptides by serum albumin proteins.<sup>21</sup>

In conclusion, we have solved the first crystal structure of a biphenyl-cross-linked peptide in complex with its target Mcl-1. Similar to the crystal structures involving hydrocarbon cross-linkers,<sup>22</sup> the biphenyl cross-linker formed an edge-to-face  $\pi$ - $\pi$  interaction with His-205 of Mcl-1, potentially contributing to tighter binding. Using the structural insights we obtained, we successfully remodeled the surface of the cross-linked peptide through residue substitution and backbone N-methylation and obtained a pair of cross-linked peptides with greatly increased helicity, cell permeability, proteolytic stability, and cell-killing activity in Mcl-1-overexpressing cancer cells. While side-chain cross-linking has become a major strategy for translating bioactive helical peptides into potential therapeutics targeting intracellular protein-protein interactions,<sup>23</sup> the work presented here illustrates the subtlety of each system and highlights the value of complementary peptide modification chemistries (e.g., N-methylation).

## ■ ASSOCIATED CONTENT

### Supporting Information

Experimental details and characterization data; complete refs 2c, 6, 12, 14, and 17. This material is available free of charge via the Internet at <http://pubs.acs.org>. The crystal structure of Mcl-1 in complex with **2** has been deposited in the Protein Data Bank as entry 4G35.

## ■ AUTHOR INFORMATION

### Corresponding Author

qinglin@buffalo.edu

## Notes

The authors declare no competing financial interest.

## ■ ACKNOWLEDGMENTS

We gratefully acknowledge the Pardee Foundation and the Oishei Foundation (to Q.L.) and the National Institutes of Health (CA82197 to H.-G.W.; GM068440 to A.M.G.) for financial support.

## ■ REFERENCES

- (1) (a) Willis, S. N.; Adams, J. M. *Curr. Opin. Cell Biol.* **2005**, *17*, 617. (b) Chen, L.; Willis, S. N.; Wei, A.; Smith, B. J.; Fletcher, J. I.; Hinds, M. G.; Colman, P. M.; Day, C. L.; Adams, J. M.; Huang, D. C. *Mol. Cell* **2005**, *17*, 393.
- (2) (a) Vaux, D. L.; Cory, S.; Adams, J. M. *Nature* **1988**, *335*, 440. (b) Minn, A. J.; Rudin, C. M.; Boise, L. H.; Thompson, C. B. *Blood* **1995**, *86*, 1903. (c) Beroukhim, R.; et al. *Nature* **2010**, *463*, 899.
- (3) Reed, J. C. *Adv. Pharmacol.* **1997**, *41*, 501.
- (4) (a) Lessene, G.; Czabotar, P. E.; Collman, P. M. *Nat. Rev. Drug Discovery* **2008**, *7*, 989. (b) Chonghaile, T. N.; Letai, A. *Oncogene* **2009**, *27*, S149.
- (5) (a) Kutzki, O.; Park, H. S.; Ernst, J. T.; Orner, B. P.; Yin, H.; Hamilton, A. D. *J. Am. Chem. Soc.* **2002**, *124*, 11838. (b) Yin, H.; Lee, G. I.; Sedey, K. A.; Kutzki, O.; Park, H. S.; Orner, B. P.; Ernst, J. T.; Wang, H. G.; Sebt, S. M.; Hamilton, A. D. *J. Am. Chem. Soc.* **2005**, *127*, 10191.
- (6) Oltersdorf, T.; et al. *Nature* **2005**, *435*, 677.
- (7) van Delft, M. F.; Wei, A. H.; Mason, K. D.; Vandenberg, C. J.; Chen, L.; Czabotar, P. E.; Willis, S. N.; Scott, C. L.; Day, C. L.; Cory, S.; Adams, J. M.; Roberts, A. W.; Huang, D. C. *Cancer Cell* **2006**, *10*, 389.
- (8) Tahir, S. K.; Wass, J.; Joseph, M. K.; Devanarayan, V.; Hessler, P.; Zhang, H.; Elmore, S. W.; Kroeger, P. E.; Tse, C.; Rosenberg, S. H.; Anderson, M. G. *Mol. Cancer Ther.* **2010**, *9*, 545.
- (9) Horne, W. S.; Boersma, M. D.; Windsor, M. A.; Gellman, S. H. *Angew. Chem., Int. Ed.* **2008**, *47*, 2853.
- (10) (a) Walensky, L. D.; Kung, A. L.; Escher, I.; Malia, T. J.; Barbuto, S.; Wright, R. D.; Wagner, G.; Verdine, G. L.; Korsmeyer, S. J. *Science* **2004**, *305*, 1466. (b) Walensky, L. D.; Pitter, K.; Morash, J.; Oh, K. J.; Barbuto, S.; Fisher, J.; Smith, E.; Verdine, G. L.; Korsmeyer, S. J. *Mol. Cell* **2006**, *24*, 199.
- (11) Wang, D.; Liao, W.; Arora, P. S. *Angew. Chem., Int. Ed.* **2005**, *44*, 6525.
- (12) (a) Inuzuka, H.; et al. *Nature* **2011**, *471*, 104. (b) Wertz, I. E.; et al. *Nature* **2011**, *471*, 110.
- (13) (a) Lin, X.; Morgan-Lappe, S.; Huang, X.; Li, L.; Zakula, D. M.; Vernetti, L. A.; Fesik, S. W.; Shen, Y. *Oncogene* **2007**, *26*, 3972. (b) Yecies, D.; Carlson, N. E.; Deng, J.; Letai, A. *Blood* **2010**, *115*, 3304.
- (14) Czabotar, P. E.; et al. *Proc. Natl. Acad. Sci. U.S.A.* **2007**, *104*, 6217.
- (15) Muppidi, A.; Wang, Z.; Li, X.; Chen, J.; Lin, Q. *Chem. Commun.* **2011**, *47*, 9396.
- (16) Refsgaard, H. H.; Jensen, B. F.; Brockhoff, P. B.; Padkjar, S. B.; Guldbrandt, M.; Christensen, M. S. *J. Med. Chem.* **2005**, *48*, 805.
- (17) (a) Biron, E.; et al. *Angew. Chem., Int. Ed.* **2008**, *47*, 2595. (b) White, T. R.; et al. *Nat. Chem. Biol.* **2011**, *7*, 810.
- (18) Pace, C. N.; Scholtz, J. M. *Biophys. J.* **1998**, *75*, 422.
- (19) Chang, C. F.; Zehfus, M. H. *Biopolymers* **1996**, *40*, 609.
- (20) (a) Bird, G. H.; Bernal, F.; Pitter, K.; Walensky, L. D. *Methods Enzymol.* **2008**, *446*, 369. (b) Madden, M. M.; Rivera Vera, C. I.; Song, W.; Lin, Q. *Chem. Commun.* **2009**, 5588.
- (21) Specific binding of Fluo-8 to homologous BSA at protein concentrations as low as 25  $\mu$ g/mL was detected by direct FP assay (see Figure S5).
- (22) (a) Stewart, M. L.; Fire, E.; Keating, A. E.; Walensky, L. D. *Nat. Chem. Biol.* **2010**, *6*, 595. (b) Baek, S.; Kutchukian, P. S.; Verdine, G. L.; Huber, R.; Holak, T. A.; Lee, K. W.; Popowicz, G. M. *J. Am. Chem. Soc.* **2012**, *134*, 103.
- (23) Verdine, G. L.; Walensky, L. D. *Clin. Cancer Res.* **2007**, *13*, 7264.